Robotica: (2021) volume 39, pp. 200–216. © The Author(s), 2020. Published by Cambridge University Press
doi:10.1017/S0263574720000314

Bi-Level Adaptive Computed-Current Impedance Controller for Electrically Driven Robots

Mohsen Jalaeian-F.*, Mohammad Mehdi Fateh and Morteza Rahimiyan

Department of Electrical and Robotic Engineering, Shahrood University of Technology, Shahrood 3619995161, Iran
E-mails: mmfateh@shahroodut.ac.ir, morteza.rahimiyan@shahroodut.ac.ir

(Accepted April 22, 2020. First published online: May 28, 2020)

SUMMARY
This paper presents a bi-level adaptive computed-current impedance controller for electrically driven robots. This study aims to reduce calculation complexities by utilizing the electrical equations of actuators, instead of the entire model of the electromechanical system. Moreover, taking the dynamical effects of mechanical parts into account through the current's feedback, external disturbances are compensated. In order to handle uncertainties, a bi-level optimization problem is formulated to obtain guaranteed stability besides the estimation convergence. An adaptation rule and its optimal tuning gain are achieved. The proposed method is applied to control of a rehabilitation robot to evaluate its performance.

KEYWORDS: Electrically driven robots (EDRs); Rehabilitation robot; Bi-level optimization problem (BLOP); Bi-level adaptive control; Impedance control.

1. Introduction

The main idea of impedance control methods (ICMs) is to enhance the desirability of transient relation between motion and force[1] while considering the dynamical interactions between a robot and its environment.[2] Muscles have the duty to adjust the mechanical impedance of human body.[2] Therefore, when the injured limbs or weak muscles are unable to accomplish their main functions, the patients need a series of rehabilitation treatments to improve the quality of their daily life.[3] Lower limb rehabilitation robots (LLRR) have been widely developed in recent years.[4] For instance, a planar parallel manipulator,[5] a sitting-type robot,[6] an articulated 3-degree-of-freedom robot,[3] an ankle rehabilitation robot,[7] and a treadmill-based bodyweight support exoskeleton (Lokomat)[8] have been developed for lower limb rehabilitation therapies. Rehabilitation and impedance control are innately interwoven. For example, the application of impedance control in a therapeutic robot for hip joint (HipBot),[9] in a parallel robot for ankle joint,[10] in a LLRR with iterative learning approaches,[11] in an assist-as-needed robots with predictive approach,[12] and hybrid impedance controller for wrist and forearm rehabilitation[13] have been addressed.

The electrically driven robots (EDRs) take the attention of control engineers due to their importance, whereas many of them are actuated by the permanent magnet direct-current motors.[3,14] In 1993, Lewis et al. considered an approximated model of these actuators to be integrated with the main dynamical model of the robots, in control design process.[15] Following that, in 2006, approximated model of the actuators was utilized to design an adaptive controller for EDRs.[16] In this pioneering

* Corresponding author. E-mail: m.jalaeian@yahoo.com

https://doi.org/10.1017/S0263574720000314 Published online by Cambridge University Press

paper, the desired current for the actuator has been computed by the help of the model and a state observer. However, the controller needed visual task-space information and encountered difficulties from computational complexity. This method has been developed later in 2014 with the elimination of acceleration measurement.[17] In 2016, Wu et al. utilized the actuator dynamics in an integrated way with the mechanical model of the robot to compute the desired current of the actuator and to obtain the control law for an LLRR.[3] However, the values of all the dynamic parameters are considered to be known accurately, which is not true in the reality. Xu et al. considered the robot parameters to be unknown, thus designed the control law with the help of robot nominal parameters and RBF neural network approximation.[18] In 2018, Ahmadi introduced another control method based on Taylor-based approximation of integrated dynamics of an EDR.[19]

In 2008, Fateh introduced the voltage control strategy (VCS) in which only the electrical equation of the motors has been considered to control the robot.[20] The basis of the VCS method roots in the fact that the dynamical effects of the entire mechanical model of an EDR can be observed in the electrical current of its actuators. In 2013, the VCS has been expanded to the impedance control approach.[21] Khoshdel et al. expanded the VCS-based impedance control method for an LLRR as an adaptive impedance force control,[22] as a variable impedance control,[14] and as a Surface Electromyography-based impedance control.[23] In 2018, a voltage-based robust impedance controller was developed using time-delay compensation.[24] Shahhosseini introduced a robust impedance VCS controller based on Fourier series for EDRs.[26] A robust adaptive impedance voltage-based controller that use function approximation techniques was developed. This way, the number of required regressor matrices was reduced, and the desired current was obtained based on the approximated dynamic of robot.[25] In addition, a voltage-based impedance model-reference robust controller for EDRs has been introduced, using fuzzy uncertainty estimator.[27]

However, the aforementioned papers either estimate/approximate the model or ignore some parts of it, which the first approach produces computational complexity and the second reduces the performance indices. Here, we introduce an altered approach that computes the desired current based on the desired impedance model.

Here, we have two optimization objectives, namely: (i) handling parameters uncertainty without disturbing the system stability and (ii) fast parameter estimation through an optimal adaptation gain. To solve this multiobjective optimization problem, we propose a bi-level optimization problem (BLOP). The mathematical relation between these two optimization models is detailed in ref. [28]. The BLOPs are formulated with Stackelberg in the context of economy,[29] and so they have been termed Stackelberg games as well.[30] The BLOPs are optimization problems with two levels; the outer problem (upper level problem) is an optimization problem with an especial constraint that itself is another optimization problem (inner problem or lower level problem).[31] This approach has been employed in a vast range of applications including predictive control as described in ref. [32], distributed stochastic model predictive control,[33] optimal autonomous architecture for uncertain processes management,[34] multiple objectives hierarchical decision making,[35] bi-level optimal control,[36] leader-follower joint optimization problems,[37] collision avoidance of unmanned aerial vehicles.[38]

In this paper, a novel bi-level adaptive computed-current impedance control method is proposed. Contributions of this study may be highlighted as follows: (1) an altered approach to computation of the independent-joint desired current based on the desired mechanical impedance is proposed. (2) A solution for the realization problem of VCS,[20] which encounters difficulties in measuring of the current derivative,[39] is proposed. (3) An impedance controller for the Electrically Driven Lower Limb Rehabilitation Robots (EDLRs) based on their passive nature is obtained. (4) An adaptive mechanism is proposed to estimate the parameter's values, since the actuators' parameters vary during the runtime due to heat and temperature.[40] (5) A novel BLOP is defined to determine the optimal values of the tuning gains of adaptation rules, which were previously determined by the trial and error in the literature.[41–43] Accordingly, an optimal robust adaptive mechanism for parameter estimation is achieved. Therefore, the parameter estimation convergence along with the Lyapunov-based stability of the closed-loop system during the estimation is guaranteed. (6) It is noteworthy that the proposed method can be even used in position control systems, since they are a specific mode of impedance control, which is termed differently in the literature as maximum-impedance mode, inactive mode, trajectory-tracking mode, or zero-admittance mode.[44]

The rest of this paper is organized as follows: in Section 2, the systems model is presented. The proposed impedance control is explained in Section 3. The problem is modeled in the presence

https://doi.org/10.1017/S0263574720000314 Published online by Cambridge University Press

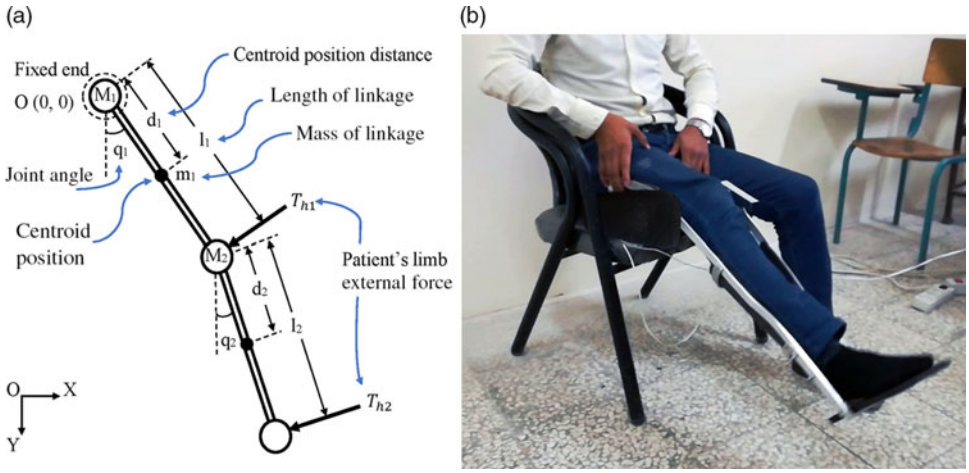


Fig. 1. (a) schematic of an LLRR, (b) the experimental setup.

of parameter uncertainty in Section 4, while Section 5 introduces a BLOP to overcome the uncertainties. Section 6 investigates the solution of the optimization problem in the proposed control design method. Section 7 addresses the implementation of the method in rehabilitation exercises. In addition, the comparison is accomplished and the results are discussed where high efficiency and superior performance of the proposed method are shown. Finally, Section 8 explains the conclusions.

2. System Dynamics

The EDR is an electromechanical system, which consists of a mechanical body including articulated links interconnected through joints, and an electrical circuit, as a part of the actuators.[3] This system has several practical considerations, which are discussed in the form of properties or assumptions during the context.

Property 1, (joint-space representation): *Since the lower limb rehabilitation tasks are defined typically in the joint space, the dynamical equations of the LLRR may be defined in the joint space as well,.*[3,14]

$$\mathbf{M_r}(\mathbf{q})\ddot{\mathbf{q}} + \mathbf{H_r}(\mathbf{q}, \dot{\mathbf{q}}) + \mathbf{T_h} + \mathbf{d_r} = \mathbf{T_r} \tag{1}$$

in which, $\mathbf{q}$ is the vector of joints angles, $\mathbf{M_r}(\mathbf{q})$ is a matrix containing the robot inertia, $\mathbf{H_r}(\mathbf{q}, \dot{\mathbf{q}})$ is a vector including centrifugal, Coriolis, and gravitational torques, $\mathbf{T_h}$ is the vector of human load torques, $\mathbf{T_r}$ is the vector of joints torque, and $\mathbf{d_r}$ is a vector containing the uncertainty included modeling imperfection, parametric uncertainties, unmodeled dynamics, friction forces, and external disturbances. Schematic and experimental setup of the LLRR are shown in Fig. 1.

Human load torque vector, $\mathbf{T_h}$, which is composed of two torques caused by human limbs dynamics and patient exerted forces, is represented by the following dynamical equations.

$$\mathbf{M_h}(\mathbf{q})\ddot{\mathbf{q}} + \mathbf{H_h}(\mathbf{q}, \dot{\mathbf{q}}) + \mathbf{T_p} + \mathbf{d_h} = \mathbf{T_h} \tag{2}$$

where, $\mathbf{T_p}$ is the torques exerted by the patient. The other parameters/variables are similar to Eq. (1), correspondingly, except that their subscripts are changed into $\mathbf{h}$ to show the relevancy with "human". The equations of motion, which describe the mechanical portion of actuators, that provides the joints torque ($\mathbf{T_r}$), are:

$$\mathbf{J_m}\ddot{\Theta}_\mathbf{m} + \mathbf{B_m}\dot{\Theta}_\mathbf{m} + \mathbf{r}\mathbf{T_r} = \mathbf{K_m}\mathbf{I} \tag{3}$$

where $\mathbf{J_m}$, $\mathbf{B_m}$, and $\mathbf{K_m}$ are the inertia, damping, and torque constant diagonal matrices, respectively, $\mathbf{\Theta_m}$ is the vector of actuators shaft angles, $\mathbf{I}$ is the vector of motors' electrical currents, and $\mathbf{r}$ is a diagonal matrix of gear reduction coefficients. Gear reduction coefficients relate the joints' velocities, ($\dot{\mathbf{q}}$), to the actuators rotational speeds ($\dot{\mathbf{\Theta}}_\mathbf{m}$) as:

$$\dot{\mathbf{q}} = \mathbf{r}\dot{\mathbf{\Theta}}_\mathbf{m} \tag{4}$$

https://doi.org/10.1017/S0263574720000314 Published online by Cambridge University Press

Based on Eqs. (1)–(4), the dynamics of complete mechanical portion of an EDR can be written as follows:

$$\mathbf{M}(\mathbf{q})\ddot{\mathbf{q}} + \mathbf{H}(\mathbf{q}, \dot{\mathbf{q}}) + \mathbf{K_m^{-1}rT_p} + \mathbf{d} = \mathbf{I} \tag{5}$$

in which,

$$\mathbf{M}(\mathbf{q}) = \mathbf{K_m^{-1}}\left(\mathbf{rM_r}(\mathbf{q}) + \mathbf{rM_h}(\mathbf{q}) + \mathbf{r^{-1}J_m}\right) \tag{6}$$

$$\mathbf{H}(\mathbf{q}, \dot{\mathbf{q}}) = \mathbf{K^{-1}}_{\mathbf{m}}\left(\mathbf{rH_r}(\mathbf{q}, \dot{\mathbf{q}}) + \mathbf{rH_h}(\mathbf{q}, \dot{\mathbf{q}}) + \mathbf{r^{-1}B_m}\dot{\mathbf{q}}\right) \tag{7}$$

$$\mathbf{d} = \mathbf{K_m^{-1}r}\left(\mathbf{d_r} + \mathbf{d_h}\right) \tag{8}$$

Furthermore, each actuator has an electrical circuit that produced the electrical current, I, as the driving input of Eq. (5), which is provided by Eq. (9).

$$L_m\dot{I} + R_m I + K_b\dot{\theta}_m = V \tag{9}$$

where L_m, R_m, and K_b are the armature inductance, resistance, and back-EMF constant, respectively, I is the electrical current, and V is the terminal voltage of the specific joint actuator. In the notation of this paper, bold characters and narrow ones represent the matrices/vectors and scalar values, respectively.

Property 2, (symmetry feature): *The total inertia matrix,* $\mathbf{M}(\mathbf{q})$*, is invertible because it is a positive-definite symmetric matrix which is uniformly bounded.*[45,46]

Based on the second property, if a new state variables vector is defined as $\mathbf{x} = [\mathbf{q}^\top, \dot{\mathbf{q}}^\top, \mathbf{I}^\top]^\top$, then the state-space representation of the dynamical equations of the EDLR can be written as:

$$\dot{\mathbf{x}} = \begin{bmatrix} \mathbf{x_2} \\ \mathbf{M}(\mathbf{x_1})^{-1}(\mathbf{x_3} - \mathbf{H}(\mathbf{x_1}, \mathbf{x_2})) \\ -\mathbf{L_m^{-1}}(\mathbf{K_b r^{-1} x_2} + \mathbf{R_m x_3}) \end{bmatrix} + \begin{bmatrix} \mathbf{0} & \mathbf{0} & \mathbf{0} \\ \mathbf{0} & -\mathbf{M}(\mathbf{x_1})^{-1}\mathbf{K_m^{-1}r} & -\mathbf{M}(\mathbf{x_1})^{-1} \\ \mathbf{L_m^{-1}} & \mathbf{0} & \mathbf{0} \end{bmatrix} \begin{bmatrix} \mathbf{V} \\ \mathbf{T_p} \\ \mathbf{d} \end{bmatrix} \tag{10}$$

This state space is a coupled nonlinear multivariable system. Control design for an EDR is a challenging task due to the combination of all these complexities, simultaneously.[3]

Property 3, (boundedness of human forces): *Human limbs can provide a limit amount of force; therefore, the patient exerted torque,* $\mathbf{T_p}$*, is bounded.*[47]

3. Impedance Control Design based on Passivity Theorem

The key role of impedance control is to drive the system to resemble the desired impedance.[11,48] However, this role is altered in different types of rehabilitation exercises, which are categorized into four main groups:[47,49] (1) range of motion or passive exercises. (2) active assistive exercises (AAEs), (3) active resistive exercises (consists of isotonic, isometric, and isokinetic trainings), and (4) manual exercises. In the AAEs, an assistive apparatus helps the patient to accomplish the task. This exercise hiddenly encourages the patient to try more without damaging his muscles.[50–52] In this study, an AAE rehabilitation training is considered in which the desired impedance rule for each joint is defined as a second-order dynamic equation:[51–53]

$$M_d(\ddot{q}_d - \ddot{q}) + B_d(\dot{q}_d - \dot{q}) + K_d(q_d - q) = K_m I + T_p \tag{11}$$

in which, M_d, B_d, and K_d are the desired impedance parameters predefined by the physiotherapist, and q_d is the desired trajectory, that is defined based on the exercise. To simplify the notation, vectors

https://doi.org/10.1017/S0263574720000314 Published online by Cambridge University Press

of desired impedance parameters (P_d), joints extended-position (Q), the desired trajectory (Q_d), and error (E) are defined as follows:

$$P_d \triangleq \left[M_d\ B_d\ K_d\right]^\top \tag{12}$$

$$Q \triangleq \left[\ddot{q}\ \dot{q}\ q\right]^\top \tag{13}$$

$$Q_d \triangleq \left[\ddot{q}_d\ \dot{q}_d\ q_d\right]^\top \tag{14}$$

$$E \triangleq Q_d - Q \triangleq \left[(\ddot{q}_d - \ddot{q})\ (\dot{q}_d - \dot{q})\ (q_d - q)\right]^\top \tag{15}$$

One can rewrite the desired impedance rule using these simplifications.

$$P_d^\top E = K_m I + T_p \tag{16}$$

Property 4, (boundedness of desired trajectory): *The desired trajectory (Q_d) is prescribed for human joint; thus, it has to be limited inside the interval of maximum range of motion (MROM); therefore, it is bounded.*[47]

Assumption 3.1. *(desired impedance parameters condition): The desired impedance parameters (P_d) are assumed to be finite real positive constants.*

Lemma 1. *(desired current definition): The desired motor current can be computed considering the satisfaction of desired impedance rule, Eq.* (16)*:*

$$I_d = K_m^{-1}(P_d^\top E - T_p) \tag{17}$$

Note that, I_d is computable, since the right-hand side of Eq. (17) is completely in hand.

Based on Lemma 1, a simple control law can be proposed for each actuator as

$$V = L_m \dot{I}_d + R_m I_d + K_b \dot{\theta}_m - L_m u \tag{18}$$

in which, u is a new control signal. Applying this control law, the closed-loop system can be obtained as a linear passive system.

$$\dot{e}_I + \frac{R_m}{L_m} e_I = u \tag{19}$$

in which, $e_I \triangleq (I_d - I)$ is the tracking error of motor current.

Remark 1. The concept of passivity theorem is detailed in ref. [54], where for a system like:

$$\begin{cases} \dot{x} = f(x, u) \\ y = h(x, u) \end{cases} \tag{20}$$

in which, $x \in R^n$ is a state vector, $u \in R^p$ and $y \in R^p$ are the input and output variables respectively, $f(.)$ and $h(.)$ are two mapping functions ($R^n \times R^p \to R^n$), which are Lipschitz and continuous, respectively, and $f(0, 0) = h(0, 0) = 0$. Now, if an energy/storage function, $F(x)$, can be found such that it is a positive semi-definite and continuously differentiable function, and also:

$$\forall (x, u), \qquad u^\top y \geq \dot{F}(x) = \frac{\partial F}{\partial x} f(x, u) \tag{21}$$

Then, the system, Eq. (20), is termed as a passive system. Since the passive systems converge to minimum energy states when there is not any other input, passivity theorem has been utilized in control design in the literature.[55–57] One can change the minimum energy states through proposing a simple proportional feedback controller like $u = -K_{di} y$, where $K_{di} = K_{di}^\top > 0$, thus, in the closed-loop

https://doi.org/10.1017/S0263574720000314 Published online by Cambridge University Press

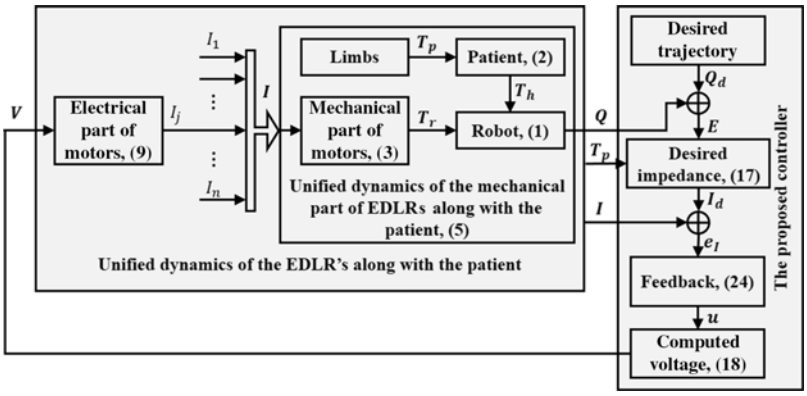


Fig. 2. Block-diagram of the proposed scheme at a glance.

system $F(x) \geq 0$, and $\dot{F}(x) \leq u^\top y = -y^\top K_{di} y \leq 0$, and the system converges to the new minimum energy states. We use this theory here in Lemma 2.

Lemma 2. *(passive closed-loop system definition): The dynamic of tracking error of motor current, which is described in Eq. (19), is a passive system.[58] To study the passivity of Eq. (19), a simple storage function is suggested.*

$$F = \frac{1}{2} {e_I}^2(t) \tag{22}$$

Differentiation of this storage function leads to:

$$\dot{F} = e_I(t)\dot{e}_I(t) = u e_I(t) - \left(\frac{R_m}{L_m}\right) {e_I}^2(t) \leqslant u e_I(t) \tag{23}$$

It confirms that the system Eq. (19) is passive;[59] therefore, to achieve a desired tracking performance, the control signal (u) can be simply a state feedback like:

$$u = \left(\frac{R_m}{L_m} - \lambda\right) e_I(t) \tag{24}$$

in which, λ is a predefined positive constant. Substituting Eq. (24) into Eq. (19), the closed-loop system can be obtained as follows:

$$\dot{e}_I(t) + \lambda e_I(t) = 0 \tag{25}$$

Solution of the closed-loop system Eq. (25) is $e_I(t) = e_I(0)e^{-\lambda t}$, which is an exponentially stable system.

Based on the introduced lemmas, the unified proposed control law is:

$$V = L_m \dot{I}_d + R_m I_d + K_b r^{-1} \dot{q} + (L_m \lambda - R_m) e_I \tag{26}$$

in which, $\dot{I}_d$ is calculated through Eulers backward differentiation approximation. $\dot{I}_d = T_s^{-1}(I_d(t) - I_d(t - T_s))$, where T_s is the sampling time of sensors.[60,61] Figure 2 illustrates the proposed scheme at a glance in a block-diagram.

4. Parameter Uncertainty Modeling

The closed-loop system, Eq. (25), is obtained by applying the proposed controller, Eq. (26), to the electrical equation of the actuators, Eq. (9). However, the parameters of the motors electrical portion may gradually vary during the time due to heat and temperatures changes; consequently, their exact values are unknown at a certain time.[40]

Assumption 4.1. *(parameters estimation): In this paper, the parameters of electrical portion are assumed unknown constants.*

https://doi.org/10.1017/S0263574720000314 Published online by Cambridge University Press

Remark 2. Though mechanical parameters may vary during time (alike electrical parameters), the closed-loop system is not sensitive to their variations because the current feedback compensates for their dynamical effects, as seen in Eq. (5).

Therefore, the proposed controller, Eq. (26), should be modified as:

$$V = \hat{L}_m \dot{I}_d + \hat{R}_m I_d + \hat{\alpha}\dot{q} + \lambda e_I \tag{27}$$

in which, $\hat{L}_m$, $\hat{R}_m$, and $\hat{\alpha}$ are the estimation of the real positive constant unknown parameters L_m, R_m, and $\alpha \triangleq K_b r^{-1}$, respectively. Applying this controller to the system, Eq. (9), we have:

$$L_m \dot{I} + R_m I + \alpha \dot{q} = \hat{L}_m \dot{I}_d + \hat{R}_m I_d + \hat{\alpha}\dot{q} + \lambda e_I \tag{28}$$

The vectors of regressors and parameters are defined as:

$$\begin{cases} \theta \triangleq \left[L_m \; R_m \; \alpha\right]^\top \\ \hat{\theta} \triangleq \left[\hat{L}_m \; \hat{R}_m \; \hat{\alpha}\right]^\top \\ Y \triangleq \left[\dot{I} \; I \; \dot{q}\right]^\top \\ Y_d \triangleq \left[\dot{I}_d \; I_d \; \dot{q}\right]^\top \end{cases} \tag{29}$$

Substituting these definitions into Eq. (28) yields:

$$\theta^\top Y = V = \hat{\theta}^\top Y_d + \lambda e_I \tag{30}$$

Subtracting $\hat{\theta}^\top Y$ from both side of Eq. (30), we have:

$$\tilde{\theta}^\top Y = \hat{\theta}^\top \tilde{Y} + \lambda e_I \tag{31}$$

in which, $\tilde{\theta} = \theta - \hat{\theta}$ and $\tilde{Y} = Y - \hat{Y}$ are estimation and tracking errors. The closed-loop system Eq. (31) is rewritten as:

$$\hat{L}_m \dot{e}_I + (\hat{R}_m + \lambda) e_I = \tilde{\theta}^\top Y \tag{32}$$

To overcome the effects of parameter uncertainty on the system stability, a BLOP is proposed.

5. Bi-Level Adaptive Optimization Approach

Single-level optimization methods cannot consider the system stability and optimal convergence of parameters estimation simultaneously in the runtime. In other words, they cannot guarantee the reduction of system tracking error and parameters estimation error at the same time. Because there is a mutual dependency between these two objectives. What is usually done in the literature is to consider only one objective. If high-performance tracking is needed, then the parameter estimation error is ignored. The main disadvantage is that although the system is stable, its dynamical behaviors are strongly dependent on the setting parameters. If the parameters are to be estimated well, then the system stability will be affected. To the best of our knowledge, currently, the setting parameters, including the adaptation gain, are set by a predetermined fixed value through a series of trial and error methods.[41–43] Predefining the setting parameters is a challenging task, because these parameters have a significant effect on the system stability, while the system condition may vary. In this paper, as an innovation, we introduce a method to find an optimal value for the adaptation gain parameter. To optimize both objectives, the two problems are to be solved iteratively. Therefore, a bi-level optimization method is proposed, in which the values of the lower level variables are assumed constant when solving the upper level problem, and the values of the upper level variables are considered to be fixed at the time of solving the lower level problem. Therefore, we do not need to predetermine the adaptation gain, and it will be adjusted online and iteratively during system runtime. At the same time, as the system has Lyapunov stability, tracking error converges to zero, and the estimated parameters converge optimally to their correct values, while they do not disturb the system stability.

https://doi.org/10.1017/S0263574720000314 Published online by Cambridge University Press

The problems of handling parameter uncertainties and tuning adaptation gain can be unified into a BLOP formulated below:

$$\min_{\hat{\theta}} \; J_1(e_I(t), \tilde{\theta}(t)) = \frac{1}{2}(\hat{L}_m {e_I}^2(t) + \tilde{\theta}(t)^\top \Omega^{-1} \tilde{\theta}(t)) \tag{33a}$$

subject to

$$\hat{L}_m \dot{e}_I(t) + (\hat{R}_m + \lambda) e_I(t) = \tilde{\theta}(t)^\top Y(t) \tag{33b}$$

$$\max_{\Omega} \; J_2\big(\tilde{\theta}(t)\big) = -\int_{\tau=t}^{\tau=t+T_w} \tilde{\theta}(\tau, \Omega)^\top \tilde{\theta}(\tau, \Omega) d\tau \tag{33c}$$

subject to

$$\Omega > 0 \tag{33d}$$

where J_1 in Eq. (33a) is a cost functional index, which provides the error reduction via $\hat{L}_m {e_I}^2(t)$, and estimation convergence through $\tilde{\theta}(t)^\top \Omega^{-1} \tilde{\theta}(t)$. The first constraint, Eq. (33b), is the closed-loop system dynamics in the presence of uncertainty, Eq. (32). Since J_2 is a value-function for Ω based on the value of estimation error through a forward moving window of length T_w, constraint Eq. (33c) maximizes this value, and finds the argument of this maximization as Ω^*. The tuning gain matrix, Ω, is diagonal and positive definite, Eq. (33d). In fact, J_2 computes the value of parameter estimation errors toward a forward moving window. This hierarchical optimization problem is termed bi-level because it is a minimization problem, which has another optimization problem inside its constraints.[28,31]

6. Solution Procedure

In order to solve the BLOP, Eqs. (33a)–(33d), it is decomposed into a master problem and a subproblem. The iterative solving of these two problems continues iteration-by-iteration until both converge to their optimal solution. A similar approach is used in [62], where Baringo used a column-and-constraint generation method[63] to solve a three-layer optimization problem. The inner problem is named the subproblem because its solution makes it possible to solve the outer problem, which is the master optimization problem (MOP). In our proposed method, the lower level variable (i.e., Ω) that is the solution of inner optimization problem, Eq. (33c), is assumed to be a known constant. Therefore, we can solve the outer optimization problem, Eq. (33a), to obtain an adaptive law for parameters estimation, Eq. (36), which is considered as a constraint for a new single-level optimization problem (i.e., Eq. (37)) based on Eq. (33c).

6.1. Master optimization problem

The MOP, Eqs. (33a)–(33b), is a relaxed representation of the original problem, Eqs. (33a)–(33d), since the tuning gain matrix, Ω, is supposed to be a fix constant during the solving process. In order to solve the MOP, based on the Lyapunov second method, the derivative of its cost function should be negative semi-definite.

$$\frac{d}{dt} J_1(e_I(t), \tilde{\theta}(t)) = \hat{L}_m e_I(t) \dot{e}_I(t) - \tilde{\theta}(t)^\top \Omega^{-1} \dot{\hat{\theta}}(t) \tag{34}$$

where θ is assumed to change very slow and can be supposed as a constant; accordingly, $\dot{\tilde{\theta}}(t) = -\dot{\hat{\theta}}(t)$. Considering the first constraint of the MOP as the closed-loop systems dynamics, Eq. (34) yields:

$$\frac{d}{dt} J_1(e_I(t), \tilde{\theta}(t)) = -(\hat{R}_m + \lambda) {e_I}^2(t) + \tilde{\theta}(t)^\top (Y(t) e_I(t) - \Omega^{-1} \dot{\hat{\theta}}(t)) \tag{35}$$

The goal is to make the left side of Eq. (35) negative. The first term of the left side is negative definite; however, the value of $\tilde{\theta}(t)$ is unknown; consequently, the coefficient of $\tilde{\theta}(t)$ must be zero.

$$\dot{\hat{\theta}}(t) = \Omega Y(t) e_I(t) \tag{36}$$

https://doi.org/10.1017/S0263574720000314 Published online by Cambridge University Press

This adaptation rule determines the value of parameters estimation iteratively. However, the values of the tuning gain (Ω) affect the performance of parameters convergence. In other words, based on Eq. (32), the reduction speed of tracking error depends on the reduction speed of the parameters estimation error, which is sensitive to the values of Ω, based on Eq. (36) . This imperfection in the adaptation rules inspired us to introduce the second-level optimization problem. In fact, in adaptive approaches, the adaptation rules guarantee the convergence of tracking error and estimation errors into zero. However, to the best of our knowledge, they do not pay attention to the optimality of this convergence.[41–43] Here, we proposed an optimal adaptive rule that guarantees the optimal convergences, by solving the subproblem.

6.2. Subproblem

Replacing the MOP, Eq. (33a), by its solution, Eq. (36), and reformulating Eqs. (33a)–(33d), we can provide the subproblem associated with the original problem as a single-level optimization problem based on $\tilde{\theta}$ over Ω. Actually, the aforementioned adaptive procedure (solution of the MOP) performs as a level reducer and changes the bi-level main problem, Eqs. (33a)–(33d), to the following single-level optimization problem, Eqs. (37a)–(37d).

$$\min_{\Omega} \; J_2(\tilde{\theta}(t)) = \int_{\tau=t}^{\tau=t+T_w} \tilde{\theta}(\tau, \Omega)^{\top} \tilde{\theta}(\tau, \Omega) d\tau \tag{37a}$$

subject to

$$\tilde{\theta}(t, \Omega)^{\top} Y(t) = \hat{\theta}(t, \Omega)^{\top} \tilde{Y}(t) + \lambda e_I(t) \tag{37b}$$

$$\dot{\tilde{\theta}}(t, \Omega) = -\Omega Y(t) e_I(t) \tag{37c}$$

$$\Omega > 0 \tag{37d}$$

The subproblem, Eqs. (33c)–(33d), evaluates the value of Ω through a forward moving window; thus, Eqs. (37a)–(37d) is a kind of predictive value-function. Solving this predictive problem in continuous time is complicated; therefore, the discrete version is

$$\min_{\Omega} \; J_2(\tilde{\theta}(k, \Omega)) = \sum_{n=k+1}^{k+N} \tilde{\theta}(n, \Omega)^{\top} \tilde{\theta}(n, \Omega) \tag{38a}$$

subject to

$$\tilde{\theta}(k, \Omega)^{\top} Y(k) = \hat{\theta}(k, \Omega)^{\top} \tilde{Y}(k) + \lambda e_I(k) \tag{38b}$$

$$\tilde{\theta}(k+1, \Omega) = \tilde{\theta}(k, \Omega) - T_s \Omega Y(k) e_I(k) \tag{38c}$$

$$\Omega > 0 \tag{38d}$$

in which, T_s is sampling time and N is the number of samples inside the forward moving window. One can consider $N = 1$; therefore, the cost function is obtained as

$$J_2\left(\tilde{\theta}(k, \Omega)\right) = \tilde{\theta}(k+1, \Omega)^{\top} \tilde{\theta}(k+1, \Omega) \tag{39}$$

Substituting Eq. (38c) in Eq. (39) yields:

$$\begin{aligned} J_2\left(\tilde{\theta}(k, \Omega)\right) &= \left(\tilde{\theta}(k, \Omega) - T_s \Omega Y(k) e_I(k)\right)^{\top} \times \left(\tilde{\theta}(k, \Omega) - T_s \Omega Y(k) e_I(k)\right) \\ &= \tilde{\theta}(k, \Omega)^{\top} \tilde{\theta}(k, \Omega) - 2 T_s e_I(k) Y(k)^{\top} \Omega^{\top} \tilde{\theta}(k, \Omega) \\ &\quad + T_s^2 e_I^2(k) Y(k)^{\top} \Omega^{\top} \Omega Y(k) \end{aligned} \tag{40}$$

To find out the optimal value of Ω, the gradient of J_2 is computed.

$$\nabla_{\Omega}(J_2) = 2 T_s e_I(k) \left(\mathbb{I}_{3\times 3} \cdot (\mathbb{1}_{3\times 1}^{\top} \otimes Y(k))\right) \left(T_s \Omega Y(k) e_I(k) - \tilde{\theta}(k)\right) \tag{41}$$

https://doi.org/10.1017/S0263574720000314 Published online by Cambridge University Press

in which, $\nabla_{\Omega}(J_2)$ is the gradient vector of the cost function J_2 over Ω, $\mathbb{I}_{3\times3} \in \mathbb{R}^{3\times3}$ is an identity matrix, the dot stands for dot product operator, $\mathbb{1}_{3\times1}^{\top}$ is a row vector of all ones, and $\otimes$ is the Kronecker tensor product operator. The Hessian matrix of the cost function, J_2, over Ω is:

$$\mathcal{H}_{\Omega}(J_2) = 2T_s^2 e_I^2(k)\Big(\mathbb{I}_{3\times3} \cdot (Y(k)^{\top} \otimes Y(k))\Big) \tag{42}$$

The Hessian, $\mathcal{H}_{\Omega}(J_2)$, is a positive definite matrix; thus, J_2 is a convex system, and the root of gradient is a global minimum. Therefore, the optimal value of Ω can be computed by putting the gradient equal to zero.

$$\Omega^* = \Big(T_s e_I(k)\big(\mathbb{I}_{3\times3} \cdot (\mathbb{1}_{3\times1}^{\top} \otimes Y(k))\big)\Big)^{-1} \Big(\mathbb{I}_{3\times3} \cdot (\mathbb{1}_{3\times1}^{\top} \otimes \tilde{\theta}(k))\Big) \tag{43}$$

Here, a simple recursive least square (RLS) method based on the equation Eq. (30) is utilized to estimate the value of unknown constant θ, bearing in mind that $Y(k)^{\top}\theta = V(k)$. The equations system of this estimator is detailed in the follows.

$$K(k) = P(k-1)Y(k)\Big(1 + Y(k)^{\top}P(k-1)Y(k)\Big)^{-1} \tag{44}$$

$$P(k) = \Big(\mathbb{I}_{3\times3} - K(k)Y(k)^{\top}\Big)P(k-1) \tag{45}$$

$$\theta_{rls}(k) = \theta_{rls}(k-1) + K(k)\Big(V(k) - Y(k)^{\top}\theta_{rls}(k-1)\Big) \tag{46}$$

in which, $K \in \mathbb{R}^{3\times1}$ and $P \in \mathbb{R}^{3\times3}$ are auxiliary matrices, where the variables are initialized by $P(0) = \mathbb{I}_{3\times3}$ and $\theta_{rls}(0) = 0_{3\times3}$. Therefore, the estimation is proposed as $\theta \approx \theta_{rls}(k)$, by which,

$$\begin{aligned}\Omega^* = &\Big(T_s e_I(k)\Big(\mathbb{I}_{3\times3} \cdot (\mathbb{1}_{3\times1}^{\top} \otimes Y(k))\Big)\Big)^{-1} \\ &\times \Big(\mathbb{I}_{3\times3} \cdot \Big(\mathbb{1}_{3\times1}^{\top} \otimes (\theta_{rls}(k) - \hat{\theta}(k, \Omega))\Big)\Big)\end{aligned} \tag{47}$$

Therefore, the following optimal adaptation rule for adjusting the parameters estimation is obtained based on the adaptation rule, Eq. (36), and the continuous time representation of optimal tuning gain, Eq. (47),

$$\dot{\hat{\theta}}(t)^* = \Omega^* Y(t) e_I(t) \tag{48}$$

6.3. Algorithm

The proposed optimal adaptive robust computed-current impedance controller is obtained through the steps below:

1. Set the initialization values of $P(0) = \mathbb{I}_{3\times3}$ and $\theta_{rls}(0) = 0_{3\times3}$.
2. Set the counter $k = 0$.
3. Estimate the $\theta_{rls}(k)$ based on Eqs. (44)–(46).
4. Compute the optimal value of tuning gain for the next sample time, $\Omega(k)^*$, based on Eq. (47).
5. Find the optimal $\hat{\theta}(t)^*$ such that the stability of closed-loop system and the correctness of parameter estimation are guaranteed, using Eq. (48).
6. Obtain the desired value of electrical current based on the desired impedance law, with the help of Eq. (17).
7. Calculate the terminal voltage of DC motors as the control signal, Eq. (27).
8. Apply the voltage to the robot, (9) and (5), and compute the tracking error, Eq. (15).
9. If $k < k_{max}$, then $k = k + 1$ and go to step 3.

Therefore, the proposed scheme consists of four main parts, namely, the desired current, Eq. (17), the voltage controller, Eq. (27), the parameter adaptation rule, Eq. (48), and the online tuning gain optimization, Eq. (47). For the sake of clarity, the proposed scheme flowchart is depicted in Fig 3.

https://doi.org/10.1017/S0263574720000314 Published online by Cambridge University Press

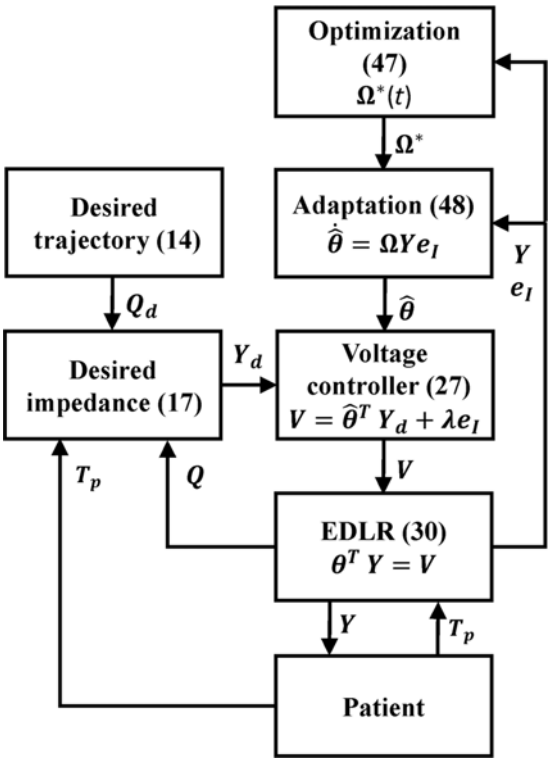


Fig. 3. The block-diagram of the system with optimal adaptive parameter estimation.

For performance evaluation of the proposed controller, it is implemented in the presence of uncertainty, which address the model imperfection, and external disturbances. The results are presented and discussed in the next section.

7. Implementation and Results

The proposed control scheme is applied to impedance control of an EDLR to provide an AAE for knee rehabilitation. To begin with, the desired trajectory for knee joint is designed in joint space, such that it makes available enough rest in each period, and it remains inside the interval of the joint MROM. In addition, the proposed desired trajectory is differentiable and smooth. The exact value of ROM for the knee joint, which is considered in the interval of $(-90°, 0)$, is derived from the available literature.[3] To perform the analysis, actual angle, speed, and acceleration of the joint are recorded, as well as the limbs exerted torque, motor voltage, and current. The desired impedance parameters are set to , $M_d = 4$, $B_d = 2$, and $K_d = 100$, as the same as.[23] Figure 4 shows the desired and actual values of the joint angle, velocity, and acceleration, in dashed and solid lines, respectively.

As seen in Fig. 4, the patients knee joint tracks the desired trajectory such that the tracking error is neglectable. Figure 5 depicts the tracking errors for better understanding.

External disturbance is applied to the robot during the seconds 70 and 90. Effect of the external disturbance on the angle, velocity, and acceleration is neglectable. This proves that the robot succeeds in helping the patient to track the desired trajectory while the mechanical impedance between robot and patient remains desired. As seen in Fig. 5, since the value of desired stiffness coefficient is big enough, the angle tracking error is neglectable, that is, less than 0.8% (less than 0.01 radian or half a degree). Patient exerted torque, desired and actual robot torques, and the torque tracking error are illustrated in Fig. 6, respectively.

As seen in Fig. 6, the robot helps the patient to conform with the desired impedance. Robot torque tracks its desired values closely such that the mean square tracking error of its tracking is less than 0.015%. In addition, it is worth noting that the effects of external disturbance are damped sufficiently. For this assistive rehabilitation, the desired and actual electrical currents are compared in Fig. 7. In addition, the current tracking error and the terminal voltage of the DCM are illustrated as well.

https://doi.org/10.1017/S0263574720000314 Published online by Cambridge University Press

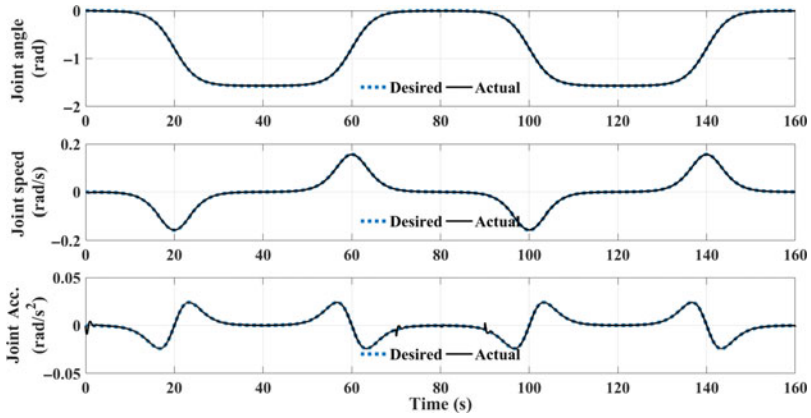


Fig. 4. Desired and actual values of the joint angle, velocity, and acceleration.

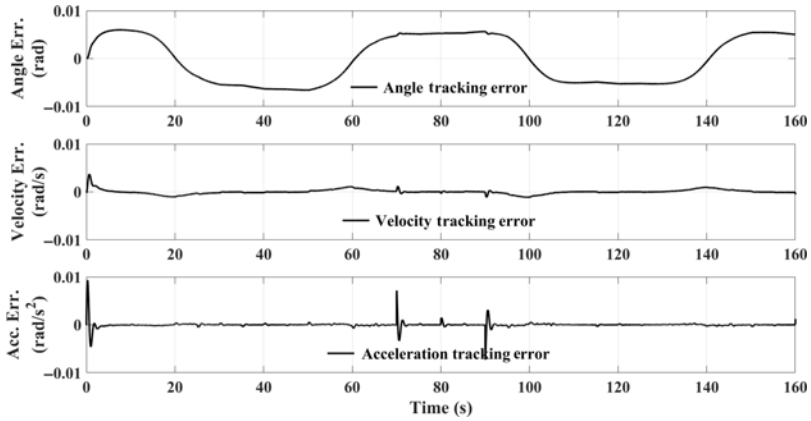


Fig. 5. Tracking error of the joint angle, velocity, and acceleration.

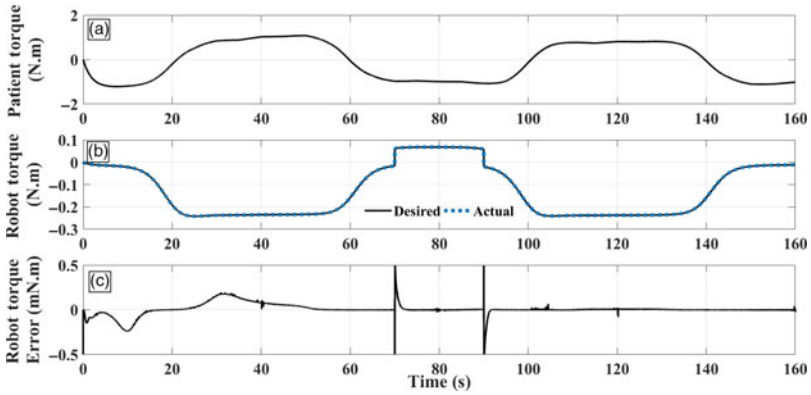


Fig. 6. (a) Patient-exerted torque, (b) desired and actual values of the robot torque, and (c) tracking error of the robot torque.

As expected, the electrical current tracks its desired trajectory perfectly, while the terminal voltage remains smooth and bounded. It is seen that the external disturbance is observable in the desired and actual curves of the current, torque, and consequently in the voltage.

As mentioned, the proposed optimization method finds an optimal value for the adaptation gain, Ω, based on the existing situation of the control system. However, its impact on the systems total performance can be studied through a comparison with the case in which the adaptation gain is determined arbitrarily (as same as the previous literatures) without online observation of the uncontrollable inputs of the system like external disturbances and patients torque. Here, we discuss this comparison. With

https://doi.org/10.1017/S0263574720000314 Published online by Cambridge University Press

Table I. Comparison study (Ω^* vs. Ω_{fix}).

Indices	Ω^*		Ω_{fix}	
	$\lambda = 5$	$\lambda = 4.5$	$\lambda = 5$	$\lambda = 4.5$
MSPEE	$7.1131e-05$	$7.4081e-05$	0.1882	0.2198
MSCTE	$6.1107e-07$	$7.7525e-07$	$9.4748e-07$	0.0117
MSITE	$2.0791e-05$	$2.0985e-05$	$2.9673e-05$	$2.0265e-04$

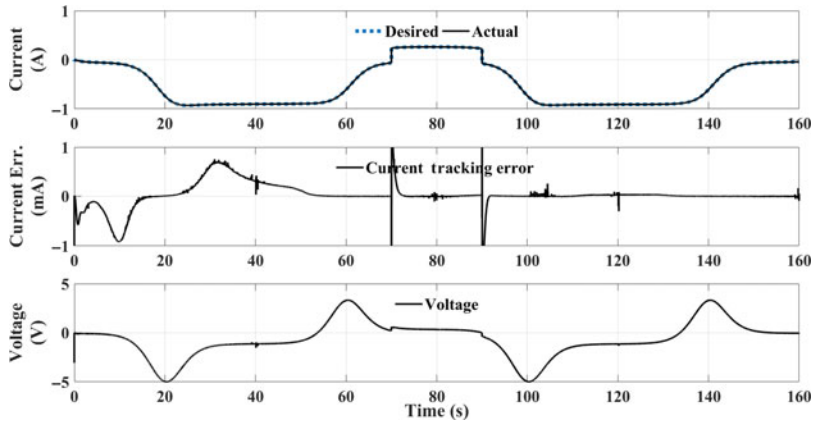


Fig. 7. Electrical current, the desired, actual, and tracking error values, and the voltage.

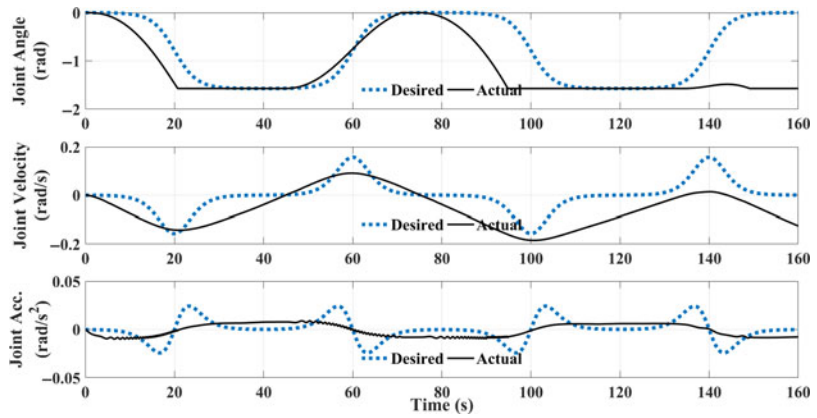


Fig. 8. Desired and actual values of the joint angle, velocity, and acceleration, without the assistive efforts.

fixed Ω, the performance is sensitive to the gain of voltage controller, λ. For instance, if the designer changes the λ from 5 to 4.5, the results of implementation are briefly reported in Table I. In which, three indices are evaluated including the mean squares of (i) parameter estimation error (MSPEE), (ii) current tracking error (MSCTE), and (iii) impedance tracking error (MSITE). The indices are reported for the proposed optimal Ω^* and fixed Ω_{fix}, each for $\lambda = 5$ and $\lambda = 4.5$.

In Table I, each column describes the results of a specific situation, and each row reports the values of an index in different situations. That was predictable that the MSE of parameter estimation error in the case of optimal Ω^* would be much better than the fixed Ω_{fix} case. Moreover, in the optimal Ω^* case, the sensitivity to every changes of other coefficients is lower than the other case (i.e., fixed Ω_{fix}). These two facts are correct about the other indices.

Moreover, to observe the effects of robot efforts, here we study the case that the robot is inactivated. The tracking performance is illustrated in Fig. 8, and the tracking error is illustrated in Fig. 9.

Without the assistance of rehabilitation robot, since the only force source is the weak limbs of patient, tracking performance decreases, that is, tracking error increases. When patients are not able to accomplish the tasks, they lose their hope and confidence. Consequently, the treatment

https://doi.org/10.1017/S0263574720000314 Published online by Cambridge University Press

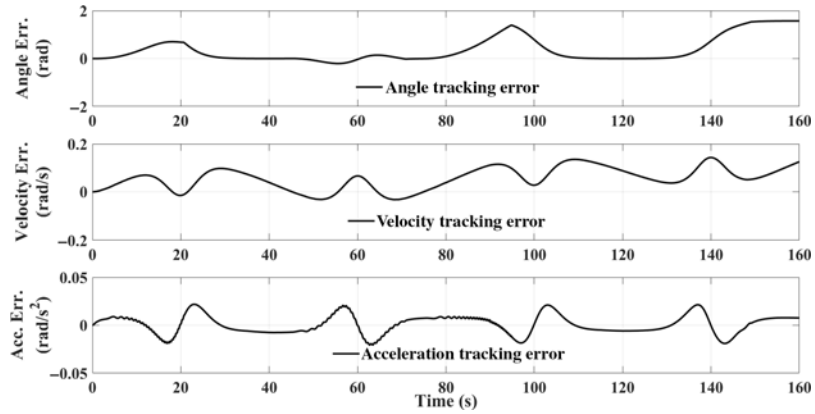


Fig. 9. Tracking error of the joint angle, velocity, and acceleration, without assistive efforts.

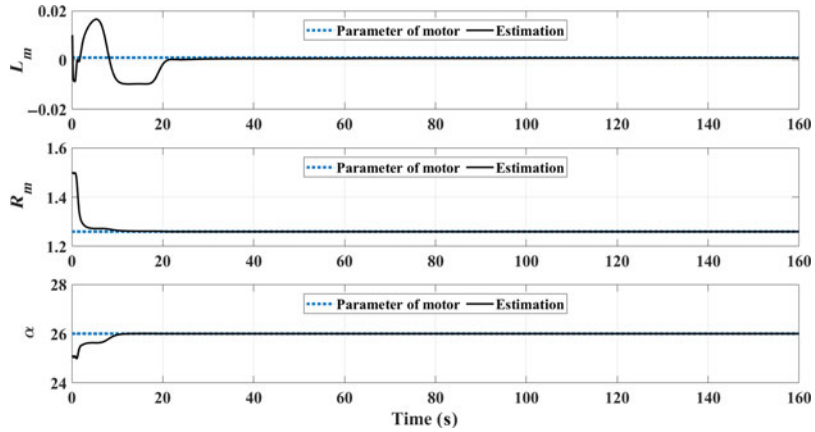


Fig. 10. Estimation convergences of the motor parameters, $\hat{\theta}^*(t)$.

process without the robots will be time consuming. The proposed controller on an EDLR in AAEs helps patient not only to track the desired trajectory but also to raise the level of their hope and determination.

Figure 10 shows the parameters estimation convergences. The optimal estimations of motor parameters converge into their correct values in approximately 20 s. Moreover, the external disturbance shows no effect on the parameter estimation. As a summary, this study provides an impedance controller based on the passivity theorem and a novel current controller for EDLRs to provide the active assistive exercises. Then, as a practical consideration, it is assumed that the motor parameters vary during time. Therefore, a BLOP is defined to guarantee the optimal convergence of parameters estimation besides the system stability. However, the literature tackles these two problems individually. On the one hand, parameter adaptation rules, e.g. Eq. (36), guarantee system stability without attention to the estimation convergence. On the other hand, recursive estimation techniques, e.g. Eqs. (44)–(46), consider the parameter estimation with no attention to the system stability. To solve this issue, we present a combinatorial method that considers system stability along with the optimal estimation convergence simultaneously, by solving Eqs. (47) and (48), iteratively. Although an incorrect estimation affects system stability, the proposed method guarantees the stability by means of the Lyapunov law in the second-level optimization. The simulation results confirm the performance of the proposed controller.

8. Conclusion

In this paper, we designed a novel bi-level adaptive computed-current impedance controller and applied it to the control of an EDLR for providing active assistive exercises. A BLOP was developed for two objectives, namely, handling the parameters uncertainty and adjusting the tuning-gain

https://doi.org/10.1017/S0263574720000314 Published online by Cambridge University Press

of adaptation. The stability of closed-loop system has been proven by the help of Lyapunov-based adaptive method, ensuring convergence of the parameters to their real values, in the presence of uncertainties. It was established that an EDLR, which employs the proposed impedance controller, is a passive dissipative system; therefore, it is controllable through a simple negative feedback. Employing the passivity theorem in impedance control design, this paper proposed a simple voltage-based controller. Without using voltage-based controller, the system model is nonlinear, complex, multivariables, which its storage functions derivative is hard to be computed, and consequently, the systems stability is hard to be guaranteed. The main merit of the proposed controller is a simple solution for these struggles. The results of implementations confirm the high performance of the controller and admirable efficiency of the proposed scheme, through small tracking errors and the optimal convergence of the parameter estimations, respectively.

References

1. P. Song, Y. Yu and X. A. Zhang, "Tutorial survey and comparison of impedance control on robotic manipulation," *Robotica* **37**(5), 801–836 (2019).
2. N. Hogan, "Impedance control: An approach to manipulation: Part I-theory," *J. Dyn. Syst. Meas. Control* **107**(1), 1–7 (1985).
3. J. Wu, J. Gao, R. Song, R. Li, Y. Li and L. Jiang, "The design and control of a 3DOF lower limb rehabilitation robot," *Mechatronics* **33**(13), 13–22 (2016).
4. W. Meng, Q. Liu, Z. Zhou, Q. Ai, B. Sheng and S. Q. Xie, "Recent development of mechanisms and control strategies for robot-assisted lower limb rehabilitation," *Mechatronics* **31**, 132–145 (2015).
5. S. Mohan, J. K. Mohanta, S. Kurtenbach, J. Paris, B. Corves and M. Huesing, "Design, development and control of a 2PRP-2PPR planar parallel manipulator for lower limb rehabilitation therapies," *Mech. Mach. Theory* **112**, 272–294 (2017).
6. J. k. Mohanta, S. Mohan, P. Deepasundar and R. Kiruba-Shankar, "Development and control of a new sitting-type lower limb rehabilitation robot," *Comput. Electr. Eng.* **67**, 330–347 (2018).
7. M. S. Ayas, I. H. Altas and E. Sahin, "Fractional order based trajectory tracking control of an ankle rehabilitation robot," *Trans. Inst. Meas. Control* **40**(2), 550–564 (2018).
8. K. van Kammen, A. M. Boonstra, L. H. V. van der Woude, C. Visscher, H. A. Reinders-Messelink and R. den Otter, "Lokomat guided gait in hemiparetic stroke patients: The effects of training parameters on muscle activity and temporal symmetry," *Disabil. Rehabil.* **11**, 1–9 (2019).
9. C. H. Guzmán-Valdivia, A. Blanco-Ortega, M. A. Oliver-Salazar, F. A. Gómez-Becerra and J. L. Carrera-Escobedo, "HipBot - The design, development and control of a therapeutic robot for hip rehabilitation," *Mechatronics* **30**, 55–64 (2015).
10. P. K. Jamwal, S. Hussain, M. H. Ghayesh and S. V. Rogozina, "Impedance control of an intrinsically compliant parallel Ankle rehabilitation robot," *IEEE Trans. Ind. Electron.* **63**(6), 3638–3647 (2016).
11. C. Guo, S. Guo, J. Ji and F. Xi, "Iterative learning impedance for lower limb rehabilitation robot," *J. Healthc. Eng.*, Article ID 6732459, 9 p. (2017). doi:10.1155/2017/6732459.
12. T. Teramae, T. Noda and J. Morimoto, "EMG-based model predictive control for physical human–robot interaction: Application for assist-as-needed control," *IEEE Robot. Autom. Lett.* **3**(1), 210–217 (2018).
13. E. Akdoğan, M. E. Aktan, A. T. Koru, M. Selçuk Arslan, M. Atlıhan and B. Kuran, "Hybrid impedance control of a robot manipulator for wrist and forearm rehabilitation: Performance analysis and clinical results," *Mechatronics* **49**, 77–91 (2018).
14. V. Khoshdel and H. Moeenfard, "Variable impedance control for rehabilitation robot using interval type-2 fuzzy logic," *Int. J. Robot. Theory Appl.* **4**(3), 46–54 (2015).
15. F. L. Lewis, D. M. Dawson and C. T. Abdallah, *Control of Robot Manipulators*, 1st edn (Prentice Hall PTR, Upper Saddle River, NJ, USA, 1993).
16. C. Liu, C. C. Cheah and J. J. E. Slotine, "Adaptive Jacobian tracking control of rigid-link electrically driven robots based on visual task-space information," *Automatica* **42**(9), 1461–1501 (2006).
17. M. Ahmadipour, A. Khayatian and M. Dehghani, "Adaptive control of rigid-link electrically driven robots with parametric uncertainties in kinematics and dynamics and without acceleration measurements," *Robotica* **32**(7), 1153–1169 (2014).
18. L. Xu, Q. Hu and Y. Zhang, "L2 performance control of robot manipulators with kinematics, dynamics and actuator uncertainties," *Int. J. Robust Nonlinear Control* **27**(6), 875–893 (2017).
19. S. M. Ahmadi and M. M. Fateh, "On the Taylor series asymptotic tracking control of robots," *Robotica* **37**(3), 405–427 (2019).
20. M. M. Fateh, "On the voltage-based control of robot manipulators," *Int. J. Control Autom. Syst.* **6**(5), 702–712 (2008).
21. M. M. Fateh and R. Babaghasabha, "Impedance control of robots using voltage control strategy," *Nonlinear Dyn.* **74**(1–2), 277–286 (2013).
22. M. M. Fateh and V. Khoshdel, "Voltage-based adaptive impedance force control for a lower-limb rehabilitation robot," *Adv. Robot.* **29**(15), 1003–1013 (2015).
23. V. Khoshdel, A. Akbarzadeh, N. Naghavi, A. Sharifnezhad and M. Souzanchi-Kashani, "sEMG-based impedance control for lower-limb rehabilitation robot," *Intell. Serv. Robot.* **11**(1), 97–108 (2017).

https://doi.org/10.1017/S0263574720000314 Published online by Cambridge University Press

24. M. Souzanchi-K., A. Arab, M. R. Akbarzadeh-T. and M. M. Fateh, "Robust impedance control of uncertain mobile manipulators using time-delay compensation," *IEEE Trans. Control Syst. Technol.* **26**(6), 1942–1953 (2018).
25. M. Shahhosseini, "Impedance control of robots using voltage control strategy revisited," *J. Mod. Process. Manuf. Prod.* **7**(1), 49–66 (2019).
26. A. Izadbakhsh, P. Kheirkhahan and S. Khorashadizadeh, "FAT-based robust adaptive control of electrically driven robots in interaction with environment," *Robotica* **37**(5), 779–800 (2019).
27. G. Nazmara, M. M. Fateh and S. M. Ahmadi, "A model-reference impedance control of robot manipulators using an adaptive fuzzy uncertainty estimator," *Int. J. Comput. Intell. Syst.* **11**(1), 979–990 (2018).
28. J. Fliege and L. N. Vicente, "Multicriteria approach to bilevel optimization," *J. Optim. Theory Appl*. **131**(2), 209–225 (2006).
29. H. von Stackelberg, *The Theory of the Market Economy*, (Oxford University Press, New York, NY, USA, 1952).
30. S. Dempe, Bilevel optimization: Theory, algorithms and applications, TU Bergakademie Freiberg (2018).
31. A. Sinha, P. Malo and K. Deb, "A review on bilevel optimization: From classical to evolutionary approaches and applications," *IEEE Trans. Evol. Comput.* **22**(2), 276–295 (2018).
32. J. H. Lee, "Model predictive control: Past, present and future", *Comput. Chem. Eng.* **23**(4–5), 667–682 (1999).
33. Y. Chen and M. Hu, "Swarm intelligence-based distributed stochastic model predictive control for transactive operation of networked building clusters", *Energy Buildi.* **198**(1), 207–215 (2019).
34. S. Saraeian, B. Shirazi and H. Motameni, "Optimal autonomous architecture for uncertain processes management", *Inf. Sci.* **501**, 84–99 (2019).
35. S. L. Tilahun, "Feasibility reduction approach for hierarchical decision making with multiple objectives", *Operat. Res. Perspect.* **6** (2019).
36. F. Benita, S. Dempe and P. Mehlitz, "Bilevel optimal control problems with pure state constraints and finite-dimensional lower level", *Soc. Indus. Appl. Math.* **26**(1), 564–588 (2016).
37. G. Du, Y. Zhang, X. Liu, R. J. Jiao, Y. Xia and Y. Li, "A review of leader-follower joint optimization problems and mathematical models for product design and development", *Int. J. Adv. Manuf. Tech.* **103**, 3405–3424 (2019).
38. E. DAmato, M. Mattei and I. Notaro, "Distributed reactive model predictive control for collision avoidance of unmanned aerial vehicles in civil airspace", *J. Intell. Robot. Syst.* **97**, 185–203 (2020).
39. A. Izadbakhsh and P. Kheirkhahan, "On the voltage-based control of robot manipulators revisited," *Int. J. Control Autom. Syst.* **16**(4), 1887–1894 (2018).
40. R. Shanmugasundram, K. M. Zakaraiah and N. Yadaiah, "Effect of parameter variations on the performance of direct current (DC) servomotor drives," *JVC/J. Vib Control* **19**(10), 1575–1586 (2013).
41. G. Tao, "Multivariable adaptive control: A survey," *Automatica* **50**(11), 2737–2764 (2014).
42. M. A. Arteaga-Pérez, J. Pliego-Jiménez and J. G. Romero, "Experimental results on the robust and adaptive control of robot manipulators without velocity measurements," *IEEE Trans. Control Syst. Tech.* (2020).
43. C. Zeng, D. Shen and J. Wang, "Adaptive learning tracking for robot manipulators with varying trial lengths," *J. Franklin Inst.* **356**(12), 5993–6014 (2019).
44. P. K. Jamwal, S. Hussain, M. H. Ghayesh and S. V. Rogozina, "Adaptive impedance control of parallel ankle rehabilitation robot," *J. Dyn. Syst. Meas. Control* **139**(11), 7 p. (2017).
45. M. W. Spong, S. Hutchinson and M. Vidyasagar, "Robot modeling and control," *IEEE Control Syst.* **26**, 113–115 (2006).
46. A. Izadbakhsh and M. M. Fateh, "Robust Lyapunov-based control of flexible-joint robots using voltage control strategy," *Arab. J. Sci. Eng.* **39**(4), 3111–3121 (2014).
47. E. Akdoğan and M. A. Adli, "The design and control of a therapeutic exercise robot for lower limb rehabilitation: Physiotherabot," *Mechatronics* **21**(3), 509–522 (2011).
48. H. Huang, D. L. Crouch, M. Liu, G. S. Sawicki and D. Wang, "A cyber expert system for auto-tuning powered prosthesis impedance control parameters," *Ann. Biomed. Eng.* **44**(5), 1613–1624 (2016).
49. T. Eiammanussakul and V. Sangveraphunsiri, "A lower limb rehabilitation robot in sitting position with a review of training activities," *J. Healthc. Eng.*, Article ID 1927807, 18 p. (2018). doi:10.1155/2018/1927807.
50. S. Hussain, P. K. Jamwal, M. H. Ghayesh and S. Q. Xie, "Assist-as-needed control of an intrinsically compliant robotic gait training orthosis," *IEEE Trans. Ind. Electron.* **64**(2), 1675–1685 (2017).
51. J. Lee, P. H. Chang and R. S. Jamisola, "Relative impedance control for dual-arm robots performing asymmetric bimanual tasks," *IEEE Trans. Ind. Electron.* **61**(7), 3786–3796 (2014).
52. H. N. Rahimi, I. Howard and L. Cui, "Neural impedance adaption for assistive human–robot interaction," *Neurocomputing* **290**, 50–59 (2018).
53. A. Taherifar, G. Vossoughi and A. S. Ghafari, "Assistive-compliant control of wearable robots for partially disabled individuals," *Control Eng. Pract.* **74**, 177–190 (2018).
54. H. K. Khalil, *Nonlinear Systems*, 3rd edn (Prentice Hall, New Jersey, 2001).
55. X. Zhang and F. L. Lewis, "Cooperative output regulation of heterogeneous multi-agent systems based on passivity," *Int. J. Syst. Sci.* **49**(16), 3418–3430 (2018).
56. Y. Zhang, S. Li, J. Zou and A. H. Khan, "A passivity-based approach for kinematic control of manipulators with constraints," *IEEE Trans. Ind. Inf.* **16**(5), 3029–3038 (2020).

https://doi.org/10.1017/S0263574720000314 Published online by Cambridge University Press

57. M. J. Kim, W. Leea, J. Y. Choic, G. Chungc, K. L. Hand, I. S. Choie, C. Ottb and W. K. Chung, "A passivity-based nonlinear admittance control with application to powered upper-limb control under unknown environmental interactions," *IEEE/ASME Trans. Mechatron.* **24**(4), 1473–1484 (2019).
58. A. Calanca, R. Muradore and P. Fiorini, "Impedance control of series elastic actuators: Passivity and acceleration-based control," *Mechatronics* **47**, 37–48 (2017).
59. H. F. N. Al-Shuka and R. Song, "Decentralized adaptive partitioned approximation control of high degrees-of-freedom robotic manipulators considering three actuator control modes," *Int. J. Dyn. Control* **7**(2), 744–757 (2018).
60. D. Zou, C. Gong and Z. Xu, "Signal detection under short-interval sampling of continuous waveforms for optical wireless scattering communication," *IEEE Trans. Wirel. Commun.* **17**(5), 3431–3443 (2018).
61. F. J. Lin, S. G. Chen and I. F. Sun, "Intelligent sliding-mode position control using recurrent wavelet fuzzy neural network for electrical power steering system," *Int. J. Fuzzy Syst.* **19**, 1344–1361 (2017).
62. A. Baringo and L. Baringo, "A stochastic adaptive robust optimization approach for the offering strategy of a virtual power plant," *IEEE Trans. Power Syst.* **32**(5), 3492–3504 (2017).
63. B. Zeng and L. Zhao, "Solving two-stage robust optimization problems using a column-and- constraint generation method," *Oper. Res. Lett.* **41**(5), 457–461 (2013).

https://doi.org/10.1017/S0263574720000314 Published online by Cambridge University Press